IEEE Access
Multidisciplinary ⋮ Rapid Review ⋮ Open Access Journal

Received 25 June 2023, accepted 21 July 2023, date of publication 25 July 2023, date of current version 2 August 2023.
Digital Object Identifier 10.1109/ACCESS.2023.3298728

RESEARCH ARTICLE

Back-EMF Decay Transient Based Identification Method of Rotor Time Constant of Inverter-Fed Induction Motors for Energy Conservation

JINGYU MA[1], WENLE SONG[1], XIANGYU HAO[1], XUYANG ZHAO[2], AND HAISEN ZHAO[2], (Senior Member, IEEE)
[1]State Grid Cangzhou Power Supply Company, Cangzhou, Heibei 061001, China
[2]School of Electrical and Electronic Engineering, North China Electric Power University, Beijing 102206, China

Corresponding author: Haisen Zhao (zhaohisen@163.com)

This work was supported in part by the Technology Project of State Grid Cangzhou Electric Supply Company under Grant KJ2021-009.

ABSTRACT Variable frequency speed regulation technology is widely used in energy-saving control systems for fan and pump loads. Replacing mechanical adjustment devices such as valves with variable frequency speed regulation can effectively reduce energy consumption. The energy-saving and speed regulation performance of induction motor variable frequency drive system based on the indirect rotor flux-oriented control (I-RFOC) heavily depends on the accuracy of rotor time constant. Traditional rotor time constant measurement methods often require the motor to be in a static state, which cannot reflect the different load conditions of the motor. In the process of stator back electromotive force decay of induction motor, the rotor side information is reflected in the change law of stator side voltage and current through flux linkage coupling. Aiming at the transient experimental phenomenon of stator winding back electromotive force decay after power is disconnected, this paper proposes a rotor time constant identification method based on curve fitting and differential evolution algorithm. The identification can be completed by measuring stator voltage and current. The influence of load, zero-sequence component and variable frequency supply conditions on the identification process is also analyzed. Finally, with a 55-kW induction motor, experimental validation is also performed to verify the proposed identification method.

INDEX TERMS Induction motors, stator back-EMF transient process, rotor flux orientation control, rotor time constant identification, differential evolution algorithm.

I. INTRODUCTION

Induction motors (IMs) are widely used in industrial fields with the advantages of high reliability, simple structure and low cost. With the development of power electronics and variable frequency speed control related technologies, vector control is widely used in induction motor drive control systems. Among them, the indirect rotor flux-oriented control (I-RFOC) based on rotor flux observation is widely adopted for its good dynamic and static performance. The directional angle of the rotor flux is obtained by integrating the sum of the slip angular velocity and the rotor angular velocity. The calculation of the slip angular velocity is related to the rotor time constant T_r. The parameter error of T_r affects the decoupling of the excitation component and the torque component, it further affects the transient characteristics of the speed and torque. Therefore, accurate rotor time constant is a prerequisite for achieving good control performance in I-RFOC. The accurate observation of the rotor flux heavily relies on the rotor time constant of the IM, and there are many difficulties in accurately measuring rotor time constant. On the one hand, the rotor side parameters are affected by factors such as temperature and frequency, and the values vary greatly under different operating conditions. On the other hand, due to the

The associate editor coordinating the review of this manuscript and approving it for publication was Jorge Esteban Rodas Benítez.

high-speed rotation of the rotor during motor operation, there is a lack of mature measurement schemes to obtain rotor side parameters.

At present, the main methods for identifying the rotor time constant include conventional experimental methods, model reference adaptation, recursive least squares, etc. In the traditional off-line identification scheme of T_r no-load and locked-rotor experiments are often used to obtain motor parameters. The off-line measurement of rotor resistance and rotor leakage inductance is required to be carried out under single-phase AC voltage, and the measurement of mutual inductance needs to be carried out under no-load conditions. The measurement of rotor side parameters by applying different kinds of current and voltage signals to detect the response of current and voltage in [1], [2], and [3] belongs to static experiments. Due to the significant differences between the experimental environment and the actual operating conditions of the motor, the accuracy of the obtained rotor time constant results is poor. The parameter identification of IM based on recursive least square method was proposed in [4] and [5], but the algorithm used second-order or third-order filters to transform voltage and current is relatively complex. An online identification method for rotor time constant based on model reference adaptive control was presented in [6], which has the advantages of easy implementation and good stability. However, the optimal adaptive parameters of this method are difficult to determine, and the influence of system regulator parameters is significant.

A method for measuring the rotor time constant based on the magnetic flux decay experiment during power outage was proposed in [7], which can use voltage data to obtain identification results. However, the influence of load and zero sequence components on the measurement experiment was ignored in the paper. At the same time, there is a lack of theoretical analysis of the identification process under variable frequency power supply, and the accuracy of the results needs to be verified.

In [8], the rotor time-constant is identified by injecting stator current with an arbitrary frequency. After a proper time to reach the steady-state condition, the test current is switched to a predefined dc level. The voltage transient is therefore analyzed, allowing the estimation of the rotor time constant. Other studies presented in [9], [10], [11], and [12] has achieved online identification of the rotor time constant, adaptive control systems require the initial parameter deviation to be within a certain range, that is, the initial value of the rotor time constant needs to be obtained. Therefore, accurate offline identification of the rotor time constant is a prerequisite for online identification.

The contribution of this paper is to propose a rotor time constant identification method for IMs based on the transient decay process of stator back-EMF. This method overcomes the shortcomings of traditional motor parameter identification experiments, which are complicated to operate and cannot reflect the real operating state of the motor. The influence of load, zero-sequence component and variable frequency supply conditions on the identification process is also analyzed. Finally, with a 55-kW induction motor, experimental validation is also performed to verify the proposed identification method.

II. BASIC PRINCIPLE OF I-RFOC

The I-FOC indirectly manages the direction of rotor flux, using feedback from rotor speed and slip frequency tuning as a function of stator current. Although I-FOC does not achieve the same dynamic performance as D-FOC, it has been implemented in most industrial applications driven by induction motors. The rotor flux angle can also be obtained through calculations based on machine parameter estimation using sensorless methods.

As a key link in I-RFOC, the main function of the rotor flux observer is to use the input speed and stator current signals to accurately observe the amplitude and phase angle of the rotor flux in real-time, which is a condition for decoupling the excitation and torque components of the stator current. The principle of I-RFOC is shown in Fig. 1.

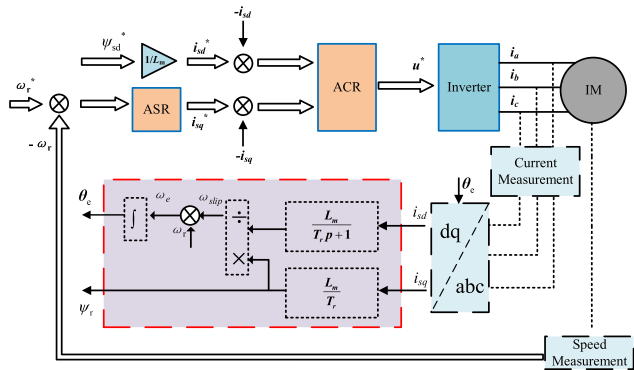

FIGURE 1. Block diagram of I-RFOC scheme.

As in Fig. 1, the accurate orientation of the rotor flux is very dependent on the motor parameters, especially the rotor time constant directly affects the dynamic tracking performance of the rotor magnetic flux electric angular velocity. If there is a deviation in the rotor time constant T_r, it will lead to inaccurate orientation of the rotor magnetic flux, which in turn causes incomplete decoupling of the stator current excitation and torque components, causing the motor torque fluctuation, and cannot obtain the expected dynamic performance [13], [14], [15].

The rotor time constant is given by

$$T_r = \frac{L_r}{R_r} = \frac{L_m + L_{lr}}{R_r} \tag{1}$$

where L_m is the excitation inductance, and the main influencing factors of L_m are the magnetic materials and geometric dimensions of the stator and rotor, as well as the influence of magnetic saturation. R_r is the rotor resistance, mainly influenced by the rotor temperature and skin effect. L_{lr} is the rotor leakage inductance.

The identification results of the T_r obtained by curve fitting in this paper reflect the state of the induction motor from the time of the stator power supply is disconnected to the end of the transient process, i.e, the T_r is considered to be a constant value in the transient process, rather than reflecting the change of the rotor time constant at each moment in real time. If the saturation near the rotor slot and the rotor skin effect are considered, higher requirements will be placed on the accuracy of data acquisition in the transient process, and it is also difficult to obtain a simple analytical expression. Therefore, the relationship between the change of rotor temperature and rotor current frequency and the change of rotor resistance and inductance is not considered when deriving the expression of stator voltage decay during the transient process.

For the convenience of analysis, the mathematical model of the induction motor is selected to be written in the two-phase rotating coordinate system with the rotor flux speed as the rotational speed, as presented in (2):

$$\begin{bmatrix} u_{sd} \\ u_{sq} \\ 0 \\ 0 \end{bmatrix} = \begin{bmatrix} R_s & & & \\ & R_s & & \\ & & R_r & \\ & & & R_r \end{bmatrix} \begin{bmatrix} i_{sd} \\ i_{sq} \\ i_{rd} \\ i_{rq} \end{bmatrix} + \begin{bmatrix} -\omega_e \psi_{sq} \\ \omega_e \psi_{sd} \\ 0 \\ \omega_{slip} \psi_r \end{bmatrix} + p \begin{bmatrix} \psi_{sd} \\ \psi_{sq} \\ \psi_r \\ 0 \end{bmatrix} \tag{2}$$

where u_{sd} and u_{sq} are the stator d-axis and q-axis voltages. R_s and R_r are the resistance of the stator and rotor windings. i_{sd}, i_{sq}, i_{rd}, and i_{rq} refer to the stator d-axis, q-axis current and rotor d-axis, q-axis current. Ψ_{sd}, Ψ_{sq}, Ψ_r represent the stator d-axis flux linkage, stator q-axis flux linkage, and rotor flux linkage; ω_e, ω_{slip}, ω_r represent the rotor flux electric angular velocity, slip electric angular velocity, and rotor electric angular velocity; p is a differential operator.

Due to the use of rotor flux orientation in the d-axis of the rotating two-phase coordinate system, the rotor flux decouples the torque component from the excitation component, i.e $\Psi_r = \Psi_{rd}$. At this point, the voltage equation of the induction motor has been simplified to a certain extent [5]. The flux equation, torque equation, and mechanical motion equation in the two-phase rotating coordinate system with rotor flux orientation are given by (3)-(5):

$$\begin{bmatrix} \psi_{sd} \\ \psi_{sq} \\ \psi_r \\ 0 \end{bmatrix} = \begin{bmatrix} L_s & 0 & L_m & 0 \\ 0 & L_s & 0 & L_m \\ L_m & 0 & L_r & 0 \\ 0 & L_m & 0 & L_m \end{bmatrix} \begin{bmatrix} i_{sd} \\ i_{sq} \\ i_{rd} \\ i_{rq} \end{bmatrix} \tag{3}$$

$$T_e = \frac{3}{2} n_p \frac{L_m}{L_r} \psi_r i_{sq} \tag{4}$$

$$T_e - T_L = \frac{J}{n_p} \frac{d\omega_r}{dt} \tag{5}$$

where L_s is the stator winding inductance. J is the rotational inertia of the motor rotor. n_p is the number of pole pairs. T_e is the electromagnetic torque. T_L is the motor load torque.

After the stator power is disconnected from the motor, due to the presence of inductance in the stator and rotor windings, a back-EMF is generated in the stator and rotor windings. During the decay process of the back-EMF, the electrical information on the rotor side can be reflected in the decay law of the stator voltage. Therefore, this process can be used to identify the rotor time constant.

In essence, the difference between the wye connection and the delta connection of the stator winding is whether to consider the zero-axis component of the stator voltage. The derivation in the two cases is similar. In order to better illustrate the process of stator back-EMF decay in the IM, an example of stator winding wye-connected squirrel cage induction motors under sinusoidal power supply is used to analyze and explain the stator back-EMF decay experiment during power outage. The experimental process is as follows: under the required identification working conditions, the motor is directly started, and the stator power is disconnected after the speed stabilizes. The data of the three-phase voltage decay process of the stator after the power outage is measured. Finally, the rotor time constant T_r is carefully identified.

III. IDENTIFICATION METHOD FOR T_r

A. CURVE FITTING METHOD

By substituting i_{sd} =0 and i_{sq} =0 into the rotor flux oriented dq rotating coordinate system induction motor model, the voltage, current, and flux relationship of the motor during the power outage process can be given as follows (6)-(8):

$$\begin{bmatrix} u_{sd} \\ u_{sq} \\ 0 \\ 0 \end{bmatrix} = \begin{bmatrix} R_s & & & \\ & R_s & & \\ & & R_r & \\ & & & R_r \end{bmatrix} \begin{bmatrix} 0 \\ 0 \\ i_{rd} \\ i_{rq} \end{bmatrix} + \begin{bmatrix} -\omega_e \psi_{sq} \\ \omega_e \psi_{sd} \\ 0 \\ \omega_{slip} \psi_r \end{bmatrix} + p \begin{bmatrix} \psi_{sd} \\ \psi_{sq} \\ \psi_r \\ 0 \end{bmatrix} \tag{6}$$

$$\begin{bmatrix} \psi_{sd} \\ \psi_{sq} \\ \psi_r \\ 0 \end{bmatrix} = \begin{bmatrix} L_s & 0 & L_m & 0 \\ 0 & L_s & 0 & L_m \\ L_m & 0 & L_r & 0 \\ 0 & L_m & 0 & L_r \end{bmatrix} \begin{bmatrix} 0 \\ 0 \\ i_{rd} \\ i_{rq} \end{bmatrix} \tag{7}$$

From the flux linkage equation, it is stated that:

$$\begin{cases} i_{rq} = 0 \\ i_{rd} = \psi_r / L_r \\ \psi_{sd} = L_m \psi_r / L_r \\ \psi_{sq} = 0 \end{cases} \tag{8}$$

Based on the voltage relationship, it is given by (9):

$$R_r \psi_r / L_r + p\psi_r = \psi_r / T_r + p\psi_r = 0 \tag{9}$$

The decay law of the rotor flux linkage can be computed as follows:

$$\psi_r(t) = \psi_{r0} e^{-t/T_r} \tag{10}$$

where Ψ_{r0} is the initial value of the rotor flux linkage at the beginning of the decay of the stator electromotive force, that is, the instantaneous value of Ψ_r before disconnecting the stator power supply. Since the phase current of the stator can be considered to change to 0 instantaneously when the stator winding is wye-connected, the voltage equation can be computed as follows:

$$\begin{cases} u_{sd} = p\psi_{sd} \\ u_{sq} = \omega_e \psi_{sd} \\ 0 = R_r i_{rd} + p\psi_r \\ 0 = R_r i_{rq} + \omega_{slip}\psi_r \end{cases} \tag{11}$$

It can be obtained from the equation for slip angle frequency in the voltage equation ω_{slip} =0, which means that after disconnecting the stator power supply, the rotor flux speed is equal to the rotor electrical angular velocity. The relationship between the stator phase voltage and the stator d-q axis voltage during the decay process of the stator back-EMF is obtained as follows:

$$e_s^2 = u_{sd}^2 + u_{sq}^2 \tag{12}$$

The influence of zero sequence component can be ignored in the case of wye-connected stator winding. Equations (9)-(11) are substituted into (12), and the stator voltage expression in the decay process is given by (13).

$$e_s^2 = k^2 \left(\frac{1}{T_r^2} + \omega_r^2 \right) e^{-\frac{2t}{T_r}} \tag{13}$$

where e_{s} is the phase voltage of stator winding, which can be measured by voltage sensor. $k = (\Psi_{\text{r0}} L_{\text{m}}/L_{\text{r}})$, considering the single identification process, it is considered that L_{m}, L_{r} Ψ_{r0} are constants, and $k$is not a function of decay time and does not affect the identification results of the rotor time constant.

After disconnecting the stator power supply, the decay waveform of phase A voltage of the stator is shown in Fig. 2. It can be seen from the envelope drawn on the measured amplitude of the stator voltage waveform that the amplitude of the stator voltage after power off decays in exponential form. It is not difficult to see from (13) that the speed of voltage amplitude decay can reflect the information of T_{r}.

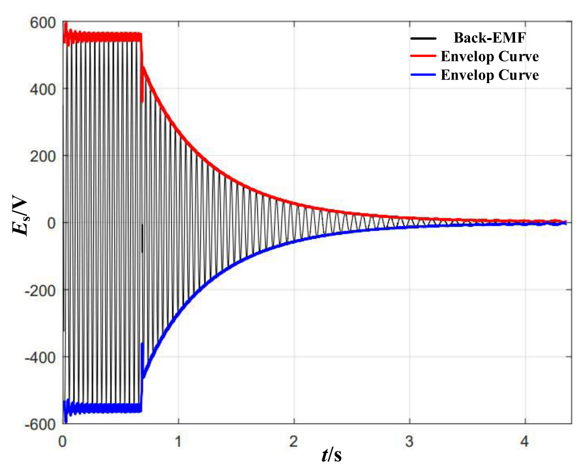

FIGURE 2. The waveform of stator back-EMF decay process.

This paper adopts a speed identification method based on frequency analysis of rotor tooth harmonic signals, which does not require the use of speed sensors and only requires the measurement of stator current to complete the identification of speed [16], [17]. The mechanical angular speed of the rotor when the IM is in steady state operation is given by (14):

$$\omega_{rm0} = \frac{2\pi}{Z_r} (f_{sh} \pm f_1) \tag{14}$$

For induction motors with wye-connected stator windings, after disconnecting the stator power supply, the stator phase current can be considered to instantly become 0. During the decay process of the stator back-EMF, the speed is also in a decay state, and the decay speed is related to the motor load situation. The rotor angular velocity can be expressed as:

$$\omega_r = n_p \left(\omega_{rm0} - \frac{T_L}{J} t \right) \tag{15}$$

where ω_{rm0} is the initial value of the rotor mechanical angular velocity during the decay of the stator back-EMF. T_{L} is the load torque, and its value is constant for constant torque load conditions. Substituting (15) into (13) can obtain the expression for the decay of the stator back-EMF as follows:

$$e_s = k\sqrt{n_p^2 \left(\omega_{rm0} - \frac{T_L}{J} \cdot t \right)^2 + (1/T_r)^2} \cdot e^{-t/T_r} \tag{16}$$

where ω_{rm0} is obtained through steady-state speed identification or speed sensors. T_{L} is the load torque, and the moment of inertia J is the mechanical parameter of the motor itself. Only k and T_{r} are unknown, and when the motor is under different load conditions, k and T_{r} may also differ. Therefore, the envelope of the measured stator voltage decay process can be fitted through this expression, so as to determine the rotor time constant of the motor.

B. IMPROVED DIFFERENTIAL EVOLUTION ALGORITHM

Differential Evolution Algorithm (DE) is a global optimization algorithm based on swarm intelligence. Each individual in the algorithm represents a solution vector. Through mutation, hybridization, competition and other operations of the population, the target function value is close to the preset value.

In traditional differential evolution algorithms, the mutation rate is often set to a fixed value, and the mutation operator is too large, making it difficult to obtain the global optimal solution. The mutation rate is small, and the diversity of the population decreases, leading to premature convergence. Improve the mutation operator by setting it as a variable that increases with the number of iterations [18], [19], it is stated that

$$F = 2^{\lambda} F_0 \tag{17}$$

where $\lambda = e^{1-\text{Gm}/(\text{Gm}-\text{G}+1)}$; G represents the number of iterations.

At the beginning of evolution, the mutation operator is $2F_0$, which can maintain the population diversity of the

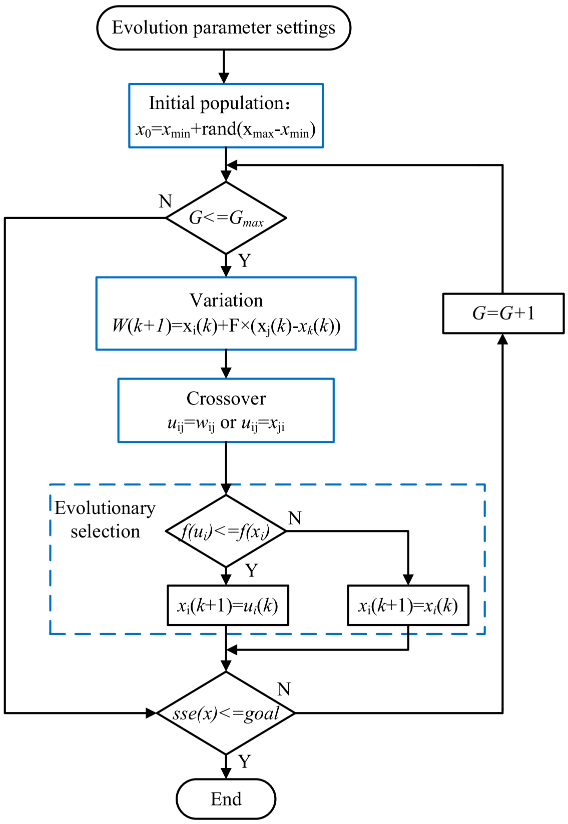

FIGURE 3. Differential evolution algorithm flowchart.

initial evolution and prevent premature convergence of the algorithm. In the later stage of evolution, the mutation operator becomes F_0, which is conducive to obtaining the solution. It is worth noting that there are some differences in the parameter identification of the motor using the differential evolution algorithm based on the steady-state data and the transient data. This is due to the fact that the rotor inertia of the induction motor must be known during the steady-state identification.

This section uses the rotor time constant identification method of differential evolution algorithm to identify the rotor time constant of the induction motor with delta-connected stator windings by measuring the stator voltage and current. The differential evolution parameters are shown in Table 1, where N is the population number, G_{max} is the maximum iteration number, E is the target error function, CR is the crossover operator, and F_0 is the initial variation factor.

TABLE 1. Differential evolution algorithm parameter settings.

Parameters	N	G_{max}	E	CR
Values	60	200	$1e^{-4}$	0.1

The identification parameter population is set to [R_s, L_{ls}, R_r, L_{lr}, L_m], and the objective function is given in (19):

$$SSE = \sum_{j=1}^{n}\left[\left(i_{s\alpha}^{*} - i_{s\alpha}\right)^2 + \left(i_{s\beta}^{*} - i_{s\beta}\right)^2 + \left(i_{s0}^{*} - i_{s0}\right)^2\right] \tag{18}$$

The parameter settings of differential evolution will affect whether the identification results can converge to the correct value, so adjustments need to be made based on the convergence of the objective function. For the case of stator winding delta-connected, due to the existence of zero sequence components, it is necessary to choose the motor state equation that considers the zero sequence component to solve the optimal parameters, as shown in (20).

$$\dot{X} = AX + BU \tag{19}$$

where equations X, A, B, U, as shown bottom of the next page.

TABLE 2. Improved differential evolution algorithm parameter identification results.

Parameters	Values	Variation range
R_s/Ω	0.1059	0.01~1
R_r/Ω	0.064	0.01~0.1
L_{ls}/mH	0.898	0.01~1
L_{lr}/mH	2.6	1~5
L_m/mH	74.19	10~100

C. INFLUENCE OF ZERO-SEQUENCE COMPONENT ON TR IDENTIFICATION

For IMs with stator winding delta connection, after disconnecting the stator power supply, the line current can be considered to instantly change to 0, and there will be zero sequence circulating current of equal amplitude and phase inside the delta-connection winding. As shown in Fig.4, there is a zero-sequence circulating current I_{s0} in the delta-connected stator winding after power off, As shown in Fig.5, the zero-sequence potential corresponding to the zero-sequence circulating current is also a part of the stator voltage decay. The left side es of (16) is the original stator phase voltage data obtained by direct measurement. Because the zero-sequence voltage u_{s0} contributes to the stator voltage, (16) needs to be corrected as (20):

$$e_s = \sqrt{k^2 n_p^2\left(\omega_{rm0} - \frac{T_L}{J}\cdot t\right)^2 + (1/T_r)^2 \cdot e^{-2t/T_r} + u_{s0}^2} \tag{20}$$

The frequency domain analysis results of the previous cycle of zero-sequence voltage attenuation are shown in Figure 5. In the frequency domain, the zero-sequence voltage corresponds to the third harmonic voltage, and the third harmonic voltage amplitude reaches 19.08 V when the stator phase voltage amplitude is 535 V.

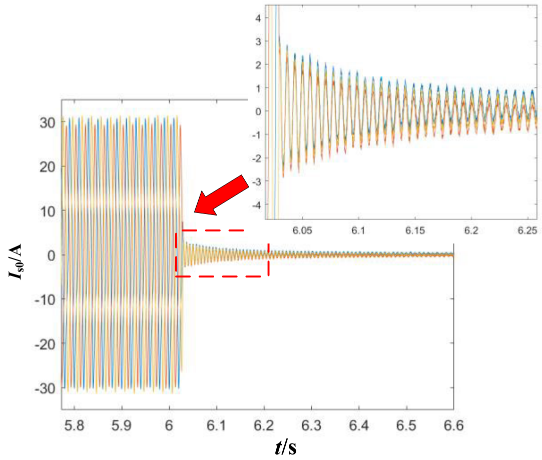

FIGURE 4. The decay process of I_{s0} in delta-connected stator winding.

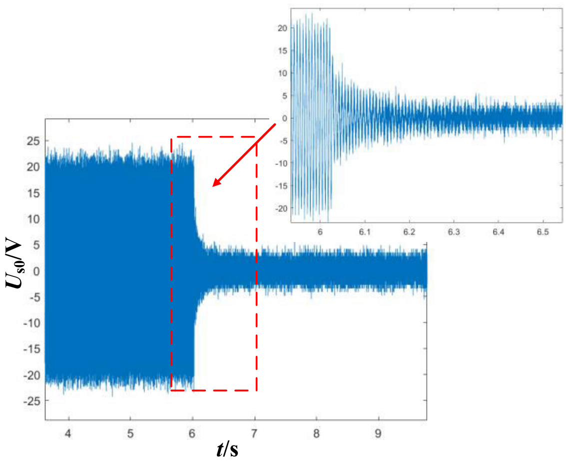

FIGURE 5. The decay process of u_{s0} in delta-connected stator winding.

D. THE IMPACT OF POWER HARMONICS

To study the effect of variable frequency power supply on the decay process of stator back-EMF, an analysis is conducted

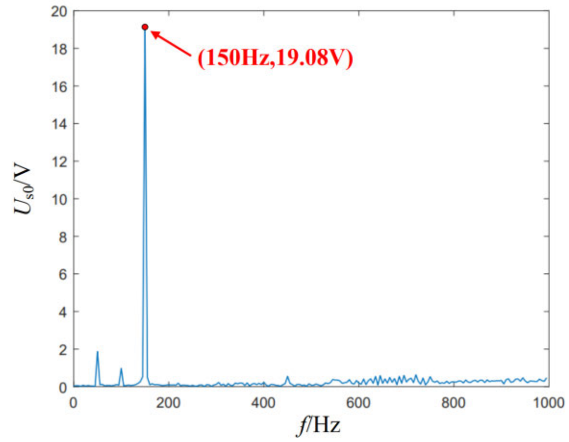

FIGURE 6. The frequency domain decomposition results of u_{s0}

on the k-th harmonic contained in the power supply. Based on the mathematical model of I-RFOC, the rotational d-q coordinate system speed is set to the rotor flux speed under the k-th harmonic power supply, and the voltage, current, and flux are also written in the form of k-th harmonic power supply. Substituting $u_{\mathrm{ksd/q}}$, $i_{\mathrm{ksd/q}}$, $i_{\mathrm{krd/q}}$, $\Psi_{\mathrm{kd/q}}$, Ψ_{kr}, ω_{ke} into the mathematical model of the motor in the rotating d-q coordinate system, following the analysis ideas in the first section, the relationship between electrical angular velocity and rotor flux linkage can be computed as follows:

$$\left(\omega_e^k - \omega_r\right)\psi_r^k = 0 \tag{21}$$

Considering that the rotor flux linkage hange abruptly, it can be concluded that $\omega_{\mathrm{e}}^{\mathrm{k}} = \omega_{\mathrm{r}}$. The physical meaning of this equation is that the power harmonics caused by variable frequency power supply do not affect the rotational speed of the rotor flux after power outage, and the rotational speed of the rotor flux generated by any order of power harmonics becomes the rotor electrical angular velocity at the moment

$$X = \left[i_{s\alpha}\ i_{s\beta}\ i_{s0}\ \psi_{r\alpha}\ \psi_{r\beta}\ \psi_{r0}\right]^T$$

$$A = \begin{bmatrix} -\frac{R_s}{\sigma L_s} - \frac{R_r L_m^2}{\sigma L_s L_r^2} & 0 & 0 & \frac{R_r L_m}{\sigma L_s L_r^2} & \omega_r \frac{L_m}{\sigma L_s L_r} & 0 \\ 0 & -\frac{R_s}{\sigma L_s} - \frac{R_r L_m^2}{\sigma L_s L_r^2} & 0 & -\omega_r \frac{L_m}{\sigma L_s L_r} & \frac{R_r L_m}{\sigma L_s L_r^2} & 0 \\ 0 & 0 & -\frac{R_s}{L_{ls}} & 0 & 0 & 0 \\ \frac{R_r L_m}{L_r} & 0 & 0 & -\frac{R_r}{L_r} & -\omega_r & 0 \\ 0 & \frac{R_r L_m}{L_r} & 0 & \omega_r & -\frac{R_r}{L_r} & 0 \\ 0 & 0 & 0 & 0 & 0 & -\frac{R_r}{L_{lr}} \end{bmatrix}$$

$$B = \begin{bmatrix} \frac{1}{\sigma L_s} & 0 & 0 & 0 & 0 \\ 0 & \frac{1}{\sigma L_s} & 0 & 0 & 0 \\ 0 & 0 & \frac{1}{L_{ls}} & 0 & 0 \end{bmatrix}^T$$

$$U = \left[U_{s\alpha}\ U_{s\beta}\ U_{s0}\right]^T$$

of power outage. Correspondingly, (16) is stated that

$$e_s^k = \frac{L_m}{L_r}\psi_r^k(0)\sqrt{\frac{1}{T_r^2}+\omega_r^2}\cdot e^{-t/T_r} \tag{22}$$

From the above equation, it can be seen that the decay process of the stator back-EMF is mainly affected by the initial value of Ψ_r and the stator voltage. For different orders of power harmonics, the stator voltage during the power outage process decays in a sinusoidal waveform with gradually decreasing amplitude. Only with different initial values of the rotor flux linkage, the decay speed of the back-EMF is the same. Therefore, the identification method for the rotor time constant is the same.

IV. EXPERIMENTATION VERIFICATION

For the rated power 55-kW induction motor with stator winding delta-connected, the rotor time constant was identified by curve fitting and differential evolution algorithm. The test bench is shown in Fig. 7.

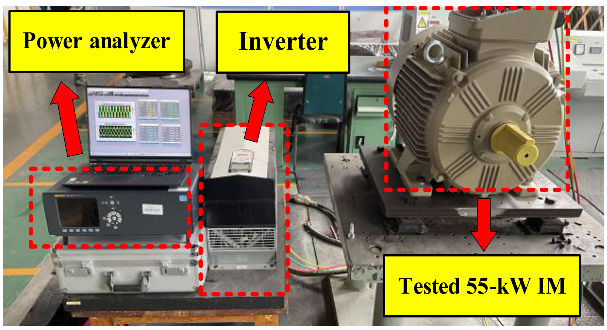

FIGURE 7. Test bench.

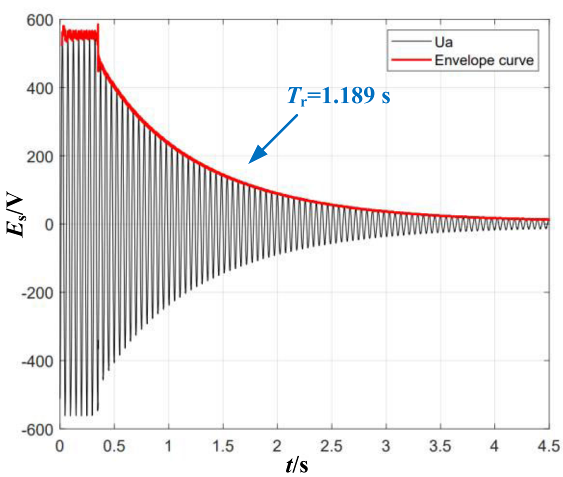

FIGURE 8. Fitting envelope of stator voltage decay process with sinusoidal supply voltage.

The decay curve of the stator back-EMF under sinusoidal power supply is shown in Fig. 8. The rotor time constant identification results can be obtained by using the fitting formula considering zero sequence components and the improved differential evolution algorithm. The convergence process of the objective error function of rotor time constant using differential evolution algorithm is shown in Fig. 9.

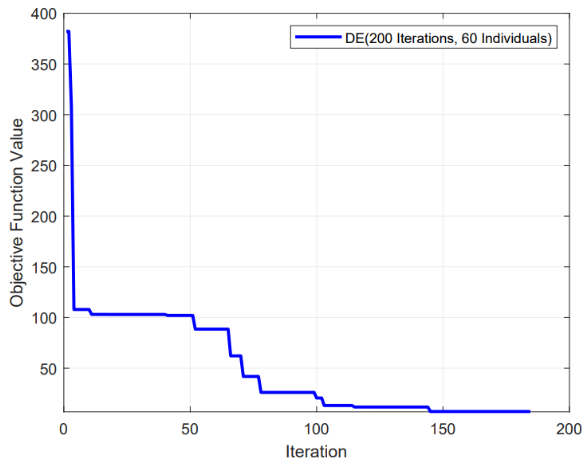

FIGURE 9. The convergence process of the objective error function of the DE algorithm with sinusoidal supply.

The envelope fitting results of the stator voltage decay process with different loads and before and after considering the zero-sequence component are shown in Figure 10. Curve A and B is the fitting result of considering the zero-sequence component and not considering the zero-sequence component when the load torque is $0.5T_N$. It can be seen that there is a certain deviation in the identification results of the rotor time constant when the zero-sequence component is not considered in (16).

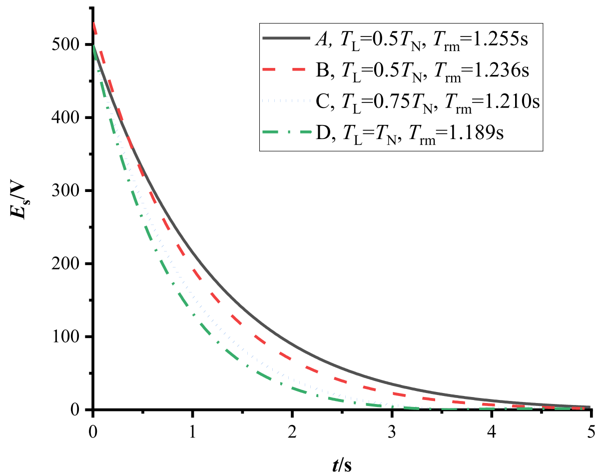

FIGURE 10. Considering the influence of zero sequence component and T_r identification results under different loads.

The curve C and D is the fitting curve when the load torque considering the influence of zero sequence component is $0.75T_N$ and T_N respectively. It can be seen from the comprehensive observation of Curve A, C and D that as the load increases, the rotor time constant identification Trm that reflect the transient process characteristics become smaller, which may be due to the fact that the rotor resistance increases with increasing temperature.

In order to verify the impact of variable frequency power supply on the decay process of stator back-EMF, SPWM variable frequency power supply was used under the same rated load conditions, and the carrier frequency of the frequency converter was set to 5 kHz. The decay process of stator back-EMF is shown in Fig. 11. It can be seen that the initial value of stator voltage decay under variable frequency power supply is 530 V, which is close to the initial value of stator voltage 535 V under sinusoidal power supply.

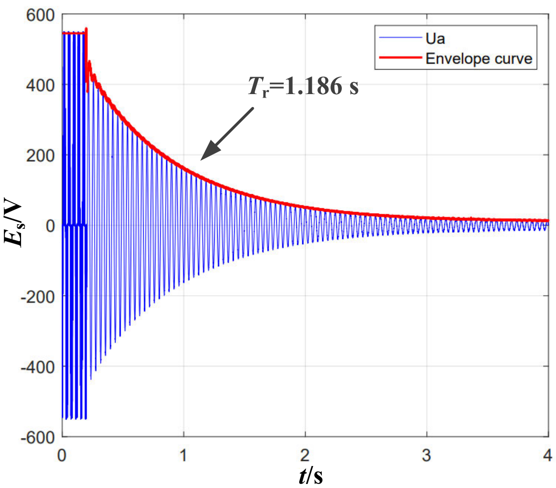

FIGURE 11. Fitting envelope of stator voltage decay process with SPWM voltage supply.

From previous analysis, it can be seen that the impact of variable frequency power supply on the decay process of stator back-EMF is mainly reflected in the initial value of rotor flux linkage, and has no impact on the identification process itself. Therefore, the identification method under variable frequency power supply is the same as the curve fitting and differential evolution algorithm under sinusoidal power supply.

The rotor time constant identification results under sinusoidal and variable frequency power supply are shown in Table 3. Method A and B refer to the methods of calculating the rotor time constant using curve fitting analytical mathematical formulas and differential evolution algorithm, respectively. SIN and SPWM refer to sinusoidal and variable frequency power supply, respectively.

The experimental results show that under the same rated load conditions, the difference in rotor time constant identification results between variable frequency power supply and sinusoidal power supply using the decay process of stator back-EMF is small. Both the curve fitting method and the differential evolution algorithm can obtain the rotor time constant parameters required for rotor flux observation.

TABLE 3. Identification results of T_r for 55kW IM under full load.

Parameters	Values	Method A (SIN)	Method A (SPWM)	Method B (SIN)	Method B (SPWM)
T_r/s	1.199	1.189	1.186	1.195	1.182
R_r/Ω	0.064	/	/	0.058	0.061
L_r/mH	76.79	/	/	69.33	72.04

The advantage of curve fitting method is that it can quickly identify the rotor time constant, and the identification accuracy is mainly affected by the accuracy of collected voltage data, but the specific parameters of rotor side resistance and inductance cannot be obtained. Its application is limited to I-RFOC. The advantage of differential evolution algorithm is that it can identify the values of R_r and L_r, so as to obtain the T_r. which can be further applied to study the variation characteristics of the rotor side parameters with load conditions. At the same time, the computational complexity is large, and it is also affected by the accuracy of collecting stator voltage and current.

V. CONCLUSION

1) This study focuses on the transient process of stator back-EMF decay in induction motors after power off, and analyzes the mathematical model of induction motors that describes the decay law of stator back-EMF. Considering the influence of load and zero sequence components on rotor time constant identification, the curve fitting method and improved differential evolution algorithm are proposed to identify the rotor time constant under sinusoidal and variable frequency power supply.

2) With a 55-kW induction motor, experimental validation was also performed to verify the proposed identification method. The experimental results show that the identification results of the rotor time constant based on the decay process of the stator back-EMF are close to the design values. Different experimental conditions are set to compare the influence of zero sequence component and load condition on rotor time constant identification. The advantages and disadvantages of the two identification methods are also compared and analyzed. The identification method for the rotor time constant of IMs based on the transient decay of stator back-EMF proposed in this study lays the foundation for the accurate orientation of the rotor flux in the I-RFOC.

REFERENCES

[1] S. R. P. Reddy and U. Loganathan, "Offline recursive identification of electrical parameters of VSI-fed induction motor drives," *IEEE Trans. Power Electron.*, vol. 35, no. 10, pp. 10711–10719, Oct. 2020.

[2] K. Wang, R. D. Lorenz, and N. A. Baloch, "Improvement of back-EMF self-sensing for induction machines when using deadbeat-direct torque and flux control," *IEEE Trans. Ind. Appl.*, vol. 53, no. 5, pp. 4569–4578, Sep. 2017.

[3] S. Foti, A. Testa, S. De Caro, T. Scimone, and M. Pulvirenti, "Sensorless field oriented control of multiple-motors fed by multiple-converters systems," in *Proc. IEEE Int. Symp. Sensorless Control Electr. Drives (SLED)*, Sep. 2017, pp. 237–242.

[4] D. Chen, W. Kong, R. Qu, and L. Zhou, "Correction of field orientation inaccuracy caused by resolver periodic error and rotor time constant variation for indirect field-oriented control induction motor drives," *IEEE Trans. Ind. Electron.*, vol. 69, no. 5, pp. 4440–4450, May 2022.
[5] P. Cao, X. Zhang, and S. Yang, "A unified-model-based analysis of MRAS for online rotor time constant estimation in an induction motor drive," *IEEE Trans. Ind. Electron.*, vol. 64, no. 6, pp. 4361–4371, Jun. 2017.
[6] P. Cao, X. Zhang, S. Yang, Z. Xie, and Y. Zhang, "Reactive-power-based MRAS for online rotor time constant estimation in induction motor drives," *IEEE Trans. Power Electron.*, vol. 33, no. 12, pp. 10835–10845, Dec. 2018.
[7] A. N. Smith, S. M. Gadoue, and J. W. Finch, "Improved rotor flux estimation at low speeds for torque MRAS-based sensorless induction motor drives," *IEEE Trans. Energy Convers.*, vol. 31, no. 1, pp. 270–282, Mar. 2016.
[8] E. Armando, A. Boglietti, S. Musumeci, and S. Rubino, "Flux-decay test: A viable solution to evaluate the induction motor rotor time-constant," *IEEE Trans. Ind. Appl.*, vol. 57, no. 4, pp. 3619–3631, Jul. 2021.
[9] S. Yang, D. Ding, X. Li, Z. Xie, X. Zhang, and L. Chang, "A novel online parameter estimation method for indirect field oriented induction motor drives," *IEEE Trans. Energy Convers.*, vol. 32, no. 4, pp. 1562–1573, Dec. 2017.
[10] A. Ferrah, K. J. Bradley, P. J. Hogben-Laing, M. S. Woolfson, G. M. Asher, M. Sumner, J. Cilia, and J. Shuli, "A speed identifier for induction motor drives using real-time adaptive digital filtering," *IEEE Trans. Ind. Appl.*, vol. 34, no. 1, pp. 156–162, Feb. 1998.
[11] S. A. Odhano, P. Pescetto, H. A. A. Awan, M. Hinkkanen, G. Pellegrino, and R. Bojoi, "Parameter identification and self-commissioning in AC motor drives: A technology status review," *IEEE Trans. Power Electron.*, vol. 34, no. 4, pp. 3603–3614, Apr. 2019.
[12] H. Zhao, H. H. Eldeeb, J. Wang, J. Kang, Y. Zhan, G. Xu, and O. A. Mohammed, "Parameter identification based online noninvasive estimation of rotor temperature in induction motors," *IEEE Trans. Ind. Appl.*, vol. 57, no. 1, pp. 417–426, Jan. 2021.
[13] V. Popovic, D. Oros, V. Vasic, and D. Marcetic, "Tuning the rotor time constant parameter of IM using the minimum order recursive linear least square estimator," *IET Electr. Power Appl.*, vol. 13, no. 2, pp. 266–276, Feb. 2019.
[14] J. Chen and J. Huang, "Stable simultaneous stator and rotor resistances identification for speed sensorless IM drives: Review and new results," *IEEE Trans. Power Electron.*, vol. 33, no. 10, pp. 8695–8709, Oct. 2018.
[15] S. Foti, A. Testa, S. De Caro, T. Scimone, and M. Pulvirenti, "Rotor flux position correction and parameters estimation on sensorless multiple induction motors drives," *IEEE Trans. Ind. Appl.*, vol. 55, no. 4, pp. 3759–3769, Jul. 2019.
[16] M. S. Zaky, M. K. Metwaly, H. Z. Azazi, and S. A. Deraz, "A new adaptive SMO for speed estimation of sensorless induction motor drives at zero and very low frequencies," *IEEE Trans. Ind. Electron.*, vol. 65, no. 9, pp. 6901–6911, Sep. 2018.
[17] H. Djadi, K. Yazid, and M. Menaa, "Parameters identification of a brushless doubly fed induction machine using pseudo-random binary signal excitation signal for recursive least squares method," *IET Electr. Power Appl.*, vol. 11, no. 9, pp. 1585–1595, Nov. 2017.
[18] G. Tarchala and T. Orlowska-Kowalska, "Equivalent-signal-based sliding mode speed MRAS-type estimator for induction motor drive stable in the regenerating mode," *IEEE Trans. Ind. Electron.*, vol. 65, no. 9, pp. 6936–6947, Sep. 2018.
[19] B. Wang, Z. Huo, Y. Yu, C. Luo, W. Sun, and D. Xu, "Stability and dynamic performance improvement of speed adaptive full-order observer for sensorless induction motor ultralow speed operation," *IEEE Trans. Power Electron.*, vol. 35, no. 11, pp. 12522–12532, Nov. 2020.

JINGYU MA received the B.E. degree in electrical engineering from North China Electric Power University (NCEPU), Beijing, China, in 2005.

He is currently a Senior Engineer (S.E.) with State Grid Cangzhou Power Supply Company, Cangzhou, China. His research interests include power grid planning and new energy access.

WENLE SONG received the M.E. degree in electrical engineering from Beijing Jiaotong University, Beijing, China, in 2013.

He is currently a Senior Engineer (S.E.) with State Grid Cangzhou Power Supply Company, Cangzhou, China. He has three provincial and ministerial level scientific and technological progress awards, authorized five invention patents, and published six papers.

XIANGYU HAO received the B.E. degree in electrical engineering from North China Electric Power University (NCEPU), Baoding, China, in 2014.

He is currently a Senior Engineer (S.E.) with State Grid Cangzhou Power Supply Company, Cangzhou, China. He has a provincial and ministerial level science and technology award, authorized three invention patents, and published three papers. His research interests include high-voltage test and transformer noise reduction.

XUYANG ZHAO received the B.E. degree from Hebei University (HBU), Hebei, China, in 2021. He is currently pursuing the master's degree with the School of Electrical and Electronic Engineering, North China Electric Power University (NCEPU).

His research interests include motor design and control and energy saving technology.

HAISEN ZHAO (Senior Member, IEEE) received the B.E. degree in agricultural electrification and automation from the Agriculture University of Hebei, Baoding, China, in 2004, and the M.E. and Ph.D. degrees in electric machines and apparatus from North China Electric Power University (NCEPU), Beijing, China, in 2007, and 2011, respectively.

He is currently a Professor with the School of Electrical and Electronic Engineering, North China Electric Power University. Moreover, he was a Visiting Scholar with the Energy Systems Research Laboratory, Department of Electrical and Computer Engineering, Florida International University (FIU), Miami, FL, USA, from December 2018 to December 2019. He is the author or coauthor of more than 100 articles in peer-reviewed journals and major international conferences. Furthermore, he has published 20 patents awarded in the areas of electric machine design, control, and energy-saving technologies. His research interests include motor design and fault diagnosis, energy-saving technologies of electric machines and drive systems, stability analysis of power system with renewable energy, and wireless power transfer.

Dr. Zhao is also a fellow of the Institute of Engineering and Technology (IET).